Acta Crystallographica Section B
Structural Science
ISSN 0108-7681

Structural filiations in the new complex titanates $SrLiMTi_4O_{11}$ (M = Cr, Fe)

I. Imaz,[a] S. Péchev,[a]* I. Koseva,[b] F. Bourée,[c] P. Gravereau,[a] P. Peshev[b] and J.-P. Chaminade[a]

[a]Institut de Chimie de la Matière Condensée de Bordeaux (ICMCB), CNRS (UPR 9048), Université Bordeaux 1, 87 Avenue du Dr A. Schweitzer, 33608 Pessac CEDEX, France, [b]Institute of General and Inorganic Chemistry, Bulgarian Academy of Sciences, Acad. G. Bonchev Str., Building 11, 1113 Sofia, Bulgaria, and [c]Laboratoire Léon Brillouin (CEA-CNRS), CEA/Saclay, 91191 Gif-sur-Yvette CEDEX, France

Correspondence e-mail: pechev@icmcb-bordeaux.cnrs.fr

Received 5 May 2006
Accepted 10 October 2006

Two new titanates of strontium, lithium and a *3d* metal, with the composition $SrLiMTi_4O_{11}$ (M = Cr, Fe), have been discovered. Single crystals were obtained by spontaneous crystallization from a high-temperature solution with $LiBO_2$ as the solvent. The structure of $SrLiCrTi_4O_{11}$ was refined in the orthorhombic space group *Pnma* (Z = 4), while $SrLiFeTi_4O_{11}$ appeared to adopt a four-times larger orthorhombic unit cell with *Pbcn* (Z = 16). The structures can be described by a close-packed arrangement of Sr and O atoms. The unit cell contains six 'compact planes' perpendicular to [100] in the layer sequence *ABACBC* [$(chc)_2$]. Ti and Cr or Fe atoms occupy some of the interstitial octahedral sites created, whereas Li atoms are in tetrahedral sites. Depending on the synthesis conditions of $SrLiCrTi_4O_{11}$, the distribution of Cr and Ti atoms on the four possible crystallographic sites is not the same. Having a similar compact-planes sequence, $SrLiCrTi_4O_{11}$ and $SrLiFeTi_4O_{11}$ structures differ in the arrangement of Sr and O atoms per layer of close packing, which also induces a correlated variation in the Li-tetrahedra distribution.

1. Introduction

In the 1920s Goldschmidt (1927) obtained and investigated the first synthetic perovskites, including the $MTiO_3$ titanates of the alkali earth metals. Among them $BaTiO_3$ was the first titanate that found an application as early as 60 years ago because of its excellent dielectric and ferroelectric properties. More recently, according to a crystallochemical scheme of ion substitution in $BaTiO_3$ proposed by Roy (1954), a large number of new phases were synthesized and various functional materials based on simple and complex perovskite titanates were developed (Wersing, 1996; Bhalla *et al.*, 2000).

Over the last decade, an increasing interest in titanates containing mobile Li ions was observed owing to their potential use in electrochemical devices and especially in rechargeable batteries (West, 1994). Three ternary oxides are known to be formed in the Li—Ti—O system:

(i) orthorhombic Li_4TiO_4 (Izquierdo & West, 1980; Gunawardane *et al.*, 1994);

(ii) monoclinic Li_2TiO_3 (Dorrian & Newnham, 1969);

(iii) ramsdellite-like $Li_2Ti_3O_7$ (Morosin & Mikkelsen Jr, 1979; Mikkelsen Jr, 1980).

In addition, a series of homogeneous solutions with cubic spinel structure, $Li_{1+x}Ti_{2-x}O_4$ ($0 \leq x \leq 0.33$) was discovered (Chen *et al.*, 2003). The promising electrochemical performances of lithium titanium ternary oxides stimulated the extension of studies to materials from systems with the additional participation of 3*d* or alkaline earth metals. Thus, the replacement of some Ti^{4+} ions by M^{3+} (M^{3+} = Cr^{3+}, Fe^{3+}, Ni^{3+})

Table 1
Crystal data and structure refinements for $SrLiM^{III}Ti_4O_{11}$ (M^{III} = Cr, Fe).

	$SrLiCrTi_4O_{11}$ Prep. 1	$SrLiCrTi_4O_{11}$ Prep. 2	$SrLiFeTi_4O_{11}$
Crystal data			
Chemical formula	$CrLiO_{11}SrTi_4$	$CrLiO_{11}SrTi_4$	$FeLiO_{11}SrTi_4$
M_r	514.16	514.16	518.01
Cell setting, space group	Orthorhombic, *Pnma*	Orthorhombic, *Pnma*	Orthorhombic, *Pbcn*
Temperature (K)	293 (2)	293 (2)	293 (2)
a, b, c (Å)	13.818 (1), 5.755 (1), 9.901 (1)	13.798 (2), 5.763 (1), 9.890 (2)	13.875 (6), 11.492 (3), 19.887 (3)
V (Å^3)	787.35 (17)	786.4 (2)	3171.1 (17)
Z	4	4	16
D_x (Mg m^{-3})	4.337	4.343	4.34
Radiation type	Mo $K\alpha$	Mo $K\alpha$	Mo $K\alpha$
μ (mm^{-1})	11.73	11.75	12.14
Crystal form, colour	Oval block, dark green	Platelet, dark green	Block, orange
Crystal size (mm)	0.09 × 0.08 × 0.07	0.05 × 0.04 × 0.01	0.08 × 0.06 × 0.06
Data collection			
Diffractometer	Nonius Kappa CCD	Nonius Kappa CCD	Nonius Kappa CCD
Data collection method	φ and ω scans	φ and ω scans	φ and ω scans
Absorption correction	Multi-scan (based on symmetry-related measurements)	Multi-scan (based on symmetry-related measurements)	Multi-scan (based on symmetry-related measurements)
T_{min}	0.35	0.55	0.38
T_{max}	0.44	0.89	0.48
No. of measured, independent and observed reflections	10 321, 1493, 1393	6546, 1243, 957	51 725, 6973, 4841
Criterion for observed reflections	$I > 2\sigma(I)$	$I > 2\sigma(I)$	$I > 2\sigma(I)$
R_{int}	0.025	0.047	0.050
θ_{max} (°)	32.0	30.0	35.0
Refinement			
Refinement hypothesis	*E*	*G*	*F*
Refinement on	F^2	F^2	F^2
$R[F^2 > 2\sigma(F^2)]$, $wR(F^2)$, S	0.023, 0.056, 1.20	0.04, 0.073, 1.18	0.053, 0.085, 1.21
No. of reflections	1393	957	4841
No. of parameters	98	98	327
Weighting scheme	$w = 1/[\sigma^2(F_o^2) + (0.0153P)^2 + 2.5599P]$, where $P = (F_o^2 + 2F_c^2)/3$	$w = 1/[\sigma^2(F_o^2) + (0.0000P)^2 + 8.8912P]$, where $P = (F_o^2 + 2F_c^2)/3$	$w = 1/[\sigma^2(F_o^2) + (0.0282P)^2 + 14.933P]$, where $P = (F_o^2 + 2F_c^2)/3$
$(\Delta/\sigma)_{max}$	0.001	<0.0001	0.002
$\Delta\rho_{max}$, $\Delta\rho_{min}$ (e Å^{-3})	0.63, −0.63	0.76, −0.74	1.54, −1.37
Extinction method	*SHELXL*	*SHELXL*	*SHELXL*
Extinction coefficient	0.0030 (3)	0.0007 (2)	0.00057 (7)

Computer programs used: *COLLECT* (Nonius BV, 1999), *DENZO-SCALEPACK* (Otwinowski & Minor, 1997), *SHELXS*97 (Sheldrick, 1997*a*), *SHELXL*97 (Sheldrick, 1997*b*).

in the spinel solid solution with x = 0.33 was reported (Robertson, Trevino, Tukamoto & Irvine, 1999) and some new electrode materials for lithium-ion batteries based on the Cr^{3+}-substituted phase were proposed (Robertson, Tukamoto & Irvine, 1999; Martin *et al.*, 2004; Sun *et al.*, 2004). The formation of the quaternary spinel oxides $LiMTiO_4$ (M = Cr, Fe), with interesting electrochemical properties, was found in the systems Li_2O–Cr_2O_3–TiO_2 (Arillo *et al.*, 1996; Garcia-Alvarado *et al.*, 2003; Kajiyama *et al.*, 2003) and Li_2O–Fe_2O_3–TiO_2 (Arillo *et al.*, 1998). A series of quaternary oxides Li_2MTiO_4 (M = Mn, Fe, Co, Ni) with rocksalt cubic structure were synthesized recently by Sebastian & Gopalakrishnan (2003), the iron compound being promising as the positive electrode for rechargeable lithium batteries (Tabuchi *et al.*, 2003).

In the literature there are several studies dealing with phase formation in the $BaO-Li_2O-TiO_2$ system. Thus, Tillmanns & Wendt (1976) reported the synthesis and crystal structure of $Ba_2Ti_{9.25}Li_3O_{22}$. Zheng *et al.* (1989) established the presence, in this system, of a new efficient Li^+-ion conductor. According to Torres-Martinez *et al.* (1994), when more than 50% TiO_2 is present in the system, two quaternary oxides with the formulae $Ba_3Li_2Ti_8O_{20}$ and $BaLi_2Ti_6O_{14}$ can be formed, the latter phase being responsible for the high Li^+ ion conductivity. More recently some of the same authors found the exact composition of the former phase to be $Ba_2Li_{2/3}Ti_{16/3}O_{13}$, and determined its structure from single-crystal X-ray diffraction data (Dussarat *et al.*, 1997).

In a recent study by the authors (Koseva *et al.*, 2002), the existence of a strontium-containing ternary titanate with the composition $SrLi_2Ti_6O_{14}$ was established. Methods for the preparation of this compound in poly- and single-crystalline form were developed and its structure was determined. In a subsequent paper (Koseva *et al.*, 2005), single crystals of $BaLi_2Ti_6O_{14}$ and $PbLi_2Ti_6O_{14}$ were grown and these oxides were shown to be isostructural with $SrLi_2Ti_6O_{14}$. Studies on the properties of strontium- and barium-containing oxides revealed the presence of Li-ion conduction in them (Nonobe

Table 2
$SrLiCrTi_4O_{11}$ reliability factors and Li and Cr/Ti U_{eq} evolution according to different hypotheses for single-crystal structure solution (*Cr-prep*1).

				U_{eq}/U_{iso} ($\times 10^4$ Å^2)				
Hypothesis	wR_2	R_1	S	Li	Site 1 4(*c*)	Site 2 4(*c*)	Site 3 4(*c*)	Site 4 8(*d*)
A					4Cr	4Ti	4Ti	8Ti
Full *hkl*	8.34	2.90	1.23	127	113	80	72	84
Sensitive hkl	*15.77*	*5.36*	*1.19*	*215*	*134*	*87*	*87*	*96*
B					4Ti	4Cr	4Ti	8Ti
Full *hkl*	9.25	2.93	1.13	139	76	124	77	88
Sensitive hkl	*13.85*	*4.62*	*1.26*	*111*	*84*	*145*	*88*	*103*
C					4Ti	4Ti	4Cr	8Ti
Full *hkl*	9.09	2.93	1.13	139	76	124	77	88
Sensitive hkl	*15.46*	*5.03*	*1.21*	*148*	*93*	*99*	*140*	*105*
D					4Ti	4Ti	4Ti	4Ti/4Cr
Full *hkl*	9.59	3.03	1.16	131	73	81	73	106
Sensitive hkl	*20.64*	*6.68*	*1.17*	*110*	*81*	*92*	*90*	*118*
E					8/3Ti/4/3Cr	8/3Ti/4/3Cr	8/3Ti/4/3Cr	8Ti
Full *hkl*	**5.61**	**2.27**	**1.20**	**128**	**86**	**95**	**86**	**84**
Sensitive hkl	***9.15***	***3.28***	***1.31***	***144***	***102***	***108***	***104***	***100***
F					3.2Ti/0.8Cr	3.2Ti/0.8Cr	3.2Ti/0.8Cr	6.4Ti/1.6Cr
Full *hkl*	6.55	2.29	1.21	131	81	90	82	84
Sensitive hkl	*11.31*	*3.94*	*1.22*	*125*	*92*	*100*	*97*	*107*
G					3.8Ti/0.2Cr	3.8Ti/0.2Cr	3.8Ti/0.2Cr	4.6Ti/3.4Cr
Full *hkl*	8.78	2.81	1.17	131	90	129	93	97
Sensitive hkl	*17.11*	*5.85*	*1.15*	*156*	*95*	*133*	*98*	*111*

et al., 2003) and the possibility of their use as an alternative anode material to the lithium titanate spinel in lithium-ion batteries (Belharouak & Amine, 2003).

The structural peculiarities of the $MLi_2Ti_6O_{14}$ (M = Sr, Ba, Pb) phases indicate various possibilities of replacing the Ti^{4+} ions by transition-metal single ions or pairs of ions. During the studies on these possibilities, some new phases were found. The present work reports the preparation and growth of single crystals of novel titanates of the systems $SrO–Li_2O–Cr_2O_3–TiO_2$ and $SrO–Li_2O–Fe_2O_3–TiO_2$ and determination of their structure with the use of single-crystal X-ray and neutron powder diffraction.

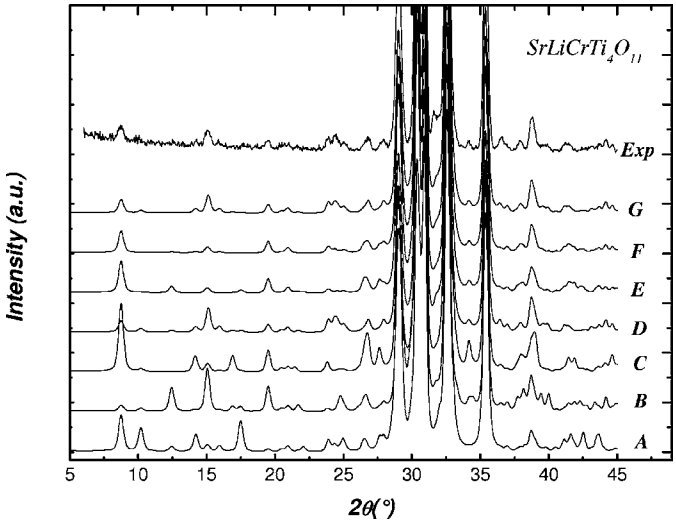

Figure 1
Simulated patterns showing the sensitivity of the neutron powder diffraction to the different site occupation. Hypotheses *A*–*G* are compared with the experimental data (Exp).

2. Experimental

2.1. Materials synthesis

2.1.1. Crystal growth. The crystals were grown from high-temperature solutions with the use of $LiBO_2$ as a solvent in a resistance furnace equipped with a *Eurotherm* controller for temperature regulation. The solutions were prepared in platinum crucibles from mixtures containing high-purity Li_2CO_3, $SrCO_3$, H_3BO_3, Cr_2O_3 (or Fe_2O_3, respectively) and TiO_2.

Solutions with the $SrO:TiO_2:LiBO_2$ molar ratio of 10:25:65 are usually used for growing $SrLi_2Ti_6O_{14}$ single crystals (Koseva *et al.*, 2002). In studies on the partial replacement of Ti by Cr, 1–6 mol% Cr_2O_3 was introduced into the solution without reducing its initial TiO_2 content. With Cr_2O_3 concentrations of up to 5 mol%, the growth of chromium-containing single crystals having the same structure as those of the parent $SrLi_2Ti_6O_{14}$ was observed. With higher concentrations of the dopant, a new kind of single crystal was obtained whose composition, established by chemical analysis (EPMA and ICP-MS), corresponded to the formula $SrLiCrTi_4O_{11}$. Later, they will be named *Cr-prep*1. The experimental density of these crystals is very close to the theoretical value for the given composition – 4.35 and 4.34 g cm^{-3}, respectively.

Experiments were carried out with the addition of the dopant Fe_2O_3 to the initial solution in concentrations which increase in steps of 5 mol% within the range 5–35 mol%. The parent $SrLi_2Ti_6O_{14}$-type structure was always preserved in the crystals grown from solutions with Fe_2O_3 concentrations of up to 20 mol%. Chemical analysis showed the insertion of iron, whose amount varied with the concentration of the dopant in the solution. When this concentration attained 25 mol% Fe_2O_3, crystals with a different structure and the composition $SrLiFeTi_4O_{11}$ appeared. The solution saturation temperature

Table 3
Atomic positions and U_{eq} for $SrLiCrTi_4O_{11}$, from *Cr-prep*1, refinement hypothesis *E*.

	Site	Site symmetry	*x*	*y*	*z*	U_{eq} (Å^2)
0.67Ti1/0.33Cr1	4(*c*)	*.m.*	0.00056 (4)	1/4	0.77081 (6)	0.0086 (1)
0.67Ti2/0.33Cr2	4(*c*)	*.m.*	0.33109 (4)	1/4	0.89031 (6)	0.0095 (1)
0.67Ti3/0.33Cr3	4(*c*)	*.m.*	0.33492 (4)	1/4	0.42830 (6)	0.0086 (1)
Ti4	8(*d*)	1	0.17189 (3)	0.00095 (7)	0.66166 (4)	0.0084 (1)
O1	4(*c*)	*.m.*	0.08656 (16)	1/4	0.6049 (2)	0.0054 (5)
O2	4(*c*)	*.m.*	0.24550 (16)	1/4	0.7430 (2)	0.0061 (4)
O3	4(*c*)	*.m.*	0.26090 (16)	1/4	0.2540 (2)	0.0056 (4)
O4	4(*c*)	*.m.*	0.39759 (16)	1/4	0.0688 (2)	0.0061 (4)
O5	4(*c*)	*.m.*	0.43363 (18)	1/4	0.5609 (2)	0.0099 (4)
O6	8(*d*)	1	0.24411 (11)	0.0018 (3)	0.99979 (16)	0.0066 (3)
O7	8(*d*)	1	0.41424 (11)	0.0065 (3)	0.32719 (16)	0.0077 (3)
O8	8(*d*)	1	0.41398 (11)	0.0275 (3)	0.81549 (15)	0.0064 (3)
Sr	4(*c*)	*.m.*	0.09472 (2)	1/4	0.10273 (3)	0.0112 (1)
Li	4(*c*)	*.m.*	0.0410 (5)	1/4	0.4217 (6)	0.0128 (12)

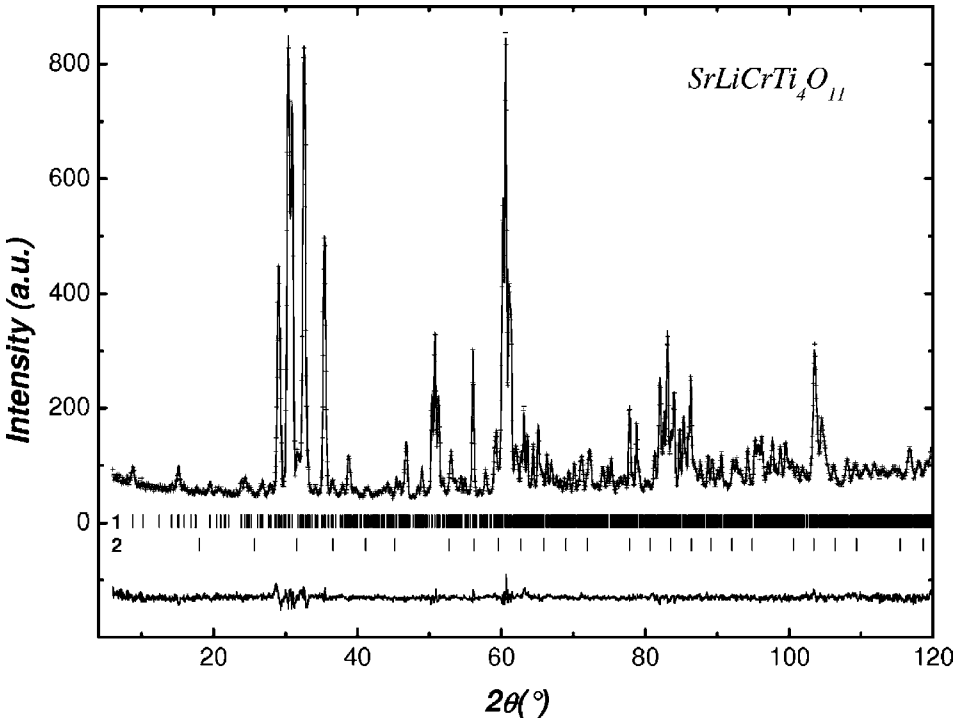

Figure 2
Final Rietveld plot with neutron diffraction of $SrLiCrTi_4O_{11}$ powder (*Cr-prep*2). The upper traces correspond to the experimental data (crosses) and the calculated pattern (solid line). The vertical ticks show the positions of the Bragg reflections for $SrLiCrTi_4O_{11}$ (1) and the impurity $SrTiO_3$ (2). The lower solid line shows the difference between experimental and calculated values.

established for this titanate was 1163 K. When the concentration of Fe_2O_3 in solution increased to *ca* 30 mol%, another new type of crystal was obtained, whose structural analysis is still in progress.

2.1.2. Powder synthesis. The solid-state synthesis of $SrLiCrTi_4O_{11}$ was successfully performed using pellets of an intimate mixture of Li_2CO_3, $SrCO_3$, H_3BO_3, Cr_2O_3 and TiO_2 in a stoichiometric ratio. The pellets were subjected to several successive heat treatments at temperatures up to 1573 K with intermediate grinding. A polycrystalline powder sample was thus obtained, referred to as *Cr-prep*2 herein.

Experiments on the synthesis of $SrLiFeTi_4O_{11}$ showed that this compound could not be obtained as a pure phase by solid state reactions. In spite of numerous thermal treatments of pellets at high temperatures (up to 1573 K), the X-ray diffraction patterns of the reaction product contained lines of the expected phase along with another phase with a perovskite-like structure plus unidentified extra lines.

2.2. Single-crystal X-ray diffraction

Single-crystal X-ray diffraction experiments were carried out on samples of $SrLiCrTi_4O_{11}$ (*Cr-prep*1), $SrLiCrTi_4O_{11}$ *(Cr-prep*2) and $SrLiFeTi_4O_{11}$. Small crystals were selected by optical examination. The measurements were performed on a Nonius Kappa CCD diffractometer with a graphite monochromator using Mo $K\alpha$ radiation. The crystal data and conditions of data collection are summarized in Table 1.[1] Both analyses of the diffraction frames and data reduction were performed by means of the *DENZO-SMN* program suite and an empirical absorption correction was applied using the *SCALEPACK* program (Otwinowski & Minor, 1997). At this stage, a test of the Laue class was performed leading to *mmm* (R_{int} values in Table 1).

The structure of $SrLiCrTi_4O_{11}$ was refined in the standard space group *Pnma*. Although the quasi-isotypical structure of $BaLi_3Ti_{9.25}O_{22}$, previously reported by Tillmanns & Wendt (1976), was solved in the non-standard space group *Pmcn*, keeping the standard space group was preferred in order to facilitate comparison with the $SrLiFeTi_4O_{11}$ structure.

2.3. Neutron powder diffraction

The neutron powder diffraction experiments were performed at room temperature at the Orphée reactor (CEA/

[1] Supplementary data for this paper are available from the IUCr electronic archives (Reference: LC5052). Services for accessing these data are described at the back of the journal.

Table 4
$SrLiCrTi_4O_{11}$: reliability factors and Li and Cr/Ti U_{eq}/U_{iso} evolution according to different hypotheses from neutron powder and X-ray single-crystal diffraction data (*Cr-prep*2).

				U_{eq}/U_{iso} ($\times 10^4$ Å^2)				
Hypothesis	wR_2 cR_{wp}	R_1R(I)	S χ^2	Li	Site 1 4(*c*)	Site 2 4(*c*)	Site 3 4(*c*)	Site 4 8(*d*)
A					4Cr	4Ti	4Ti	8Ti
X-ray (single-crystal)	11.88	4.20	1.07	147	137	91	79	47
Neutrons (powder)	*12.2*	*8.1*	*7.0*	*12 (7)*	*>10000 (divergence)*	*−40*	*00*	*2200*
B					4Ti	4Cr	4Ti	8Ti
X-ray (single-crystal)	13.05	4.10	1.08	145	80	150	80	49
Neutrons (powder)	*9.8*	*6.2*	*4.4*	*90*	*50*	*4600*	*40*	*1500*
C					4Ti	4Ti	4Cr	8Ti
X-ray (single-crystal)	12.75	4.11	1.11	142	78	91	137	47
Neutrons (powder)	*10.9*	*7.0*	*5.4*	*25*	*40*	*00*	*6000*	*2100*
D					4Ti	4Ti	4Ti	4Ti/4Cr
X-ray (single-crystal)	7.44	4.08	1.17	145	69	79	70	67
Neutrons (powder)	*6.8*	*3.5*	*2.2*	*50*	*145*	*80*	*65*	*−40*
E					8/3Ti/4/3Cr	8/3Ti/4/3Cr	8/3Ti/4/3Cr	8Ti
X-ray (single-crystal)	9.51	4.58	1.20	162	94	105	96	41
Neutrons (powder)	*9.9*	*6.6*	*4.6*	*50*	*−400*	*−300*	*−350*	*−900*
F					3.2Ti/0.8Cr	3.2Ti/0.8Cr	3.2Ti/0.8Cr	6.4Ti/1.6Cr
X-ray (single-crystal)	7.43	4.18	1.20	154	84	94	85	49
Neutrons (powder)	*7.7*	*4.6*	*2.8*	*40*	*−150*	*−100*	*−125*	*900*
G					**3.8Ti/0.2Cr**	**3.8Ti/0.2Cr**	**3.8Ti/0.2Cr**	**4.6Ti/3.4Cr**
X-ray (single-crystal)	**7.28**	**4.02**	**1.18**	**147**	**73**	**83**	**73**	**63**
Neutrons (powder)	***6.5***	***3.2***	***2.0***	***40***	***70***	***60***	***50***	***100***

Saclay, France) with the use of the two-axis high-resolution diffractometer 3T2 (λ = 0.1225 nm). The Rietveld method for structure refinement was applied, using the *Fullprof* suite of programs (Rodriguez-Carvajal, 1990; Roisnel & Rodriguez-Carvajal, 2001).

3. Structure of $SrLiCrTi_4O_{11}$

3.1. Solution with X-ray and single-crystal *Cr-prep*1

The structure of $SrLiCrTi_4O_{11}$ was solved by Patterson function deconvolution and the heavy-atoms method in the centrosymmetric space group *Pnma*. One site for Sr and four

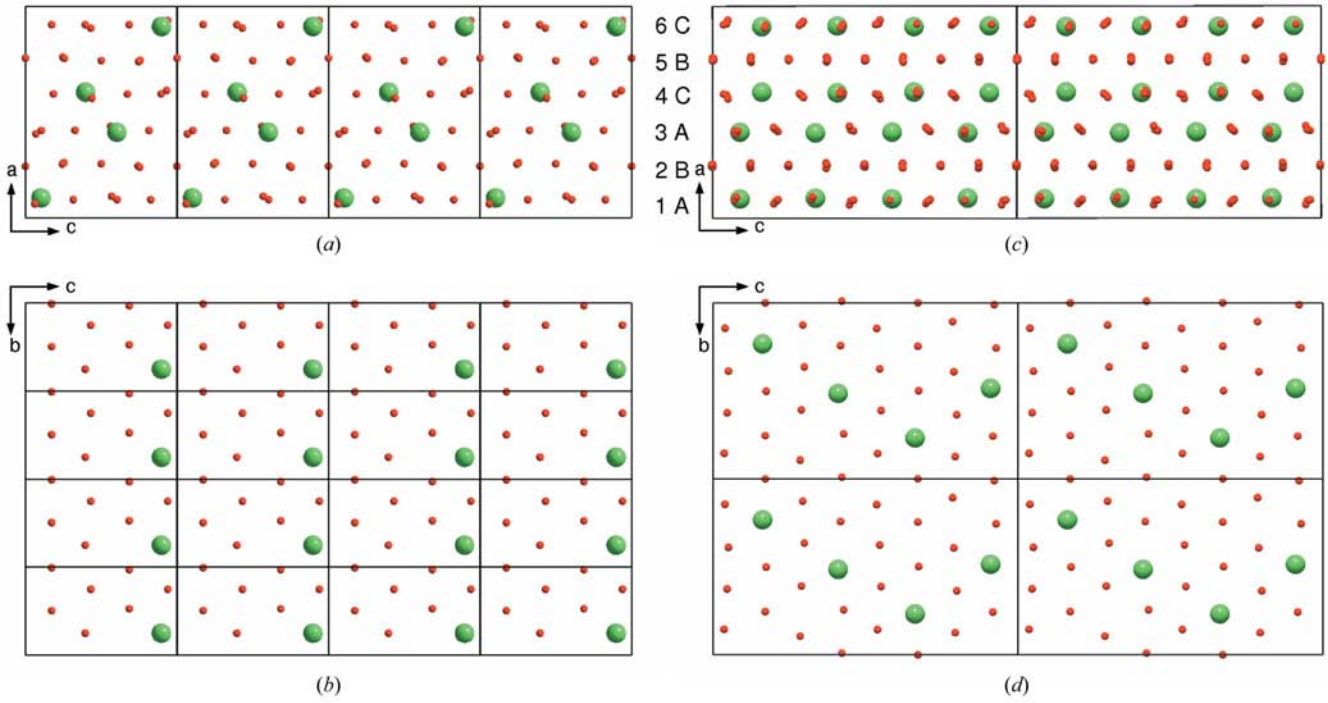

Figure 3
Close-packing arrangement for $SrLiCrTi_4O_{11}$ (Figs. 3*a* and *b*) and $SrLiFeTi_4O_{11}$ (Figs. 3*c* and *d*): (*a*) and (*c*), compact planes 'O' and 'Sr—O' sequence along the *a* axis; (*b*) and (*d*), compact plane 'Sr—O' (6-C)

sites for the two transition element atoms were located using the *SHELXS*97 program (Sheldrick, 1997*a*). The positions of the O and Li atoms were determined by refinement and successive Fourier-difference functions with the *SHELXL*97 program (Sheldrick, 1997*b*). The cationic scattering factors Sr^{2+}, Li^{+}, Ti^{4+} and Cr^{3+} were used during the refinement process.

However, the precise distribution of the Ti and Cr atoms over the four sites (three fourfold and one eightfold) was rather uncertain because of the closeness of the X-ray scattering factors of these two elements. The initial refinement considering a constrained Ti/Cr ratio on any of the possible sites with respect to the global electronegativity turned out to be unstable with large e.s.d.s for the occupancy and displacement parameters. Therefore, several simplified models of cationic distribution were introduced.

Seven different hypotheses about the occupation of the sites by Ti and Cr atoms were examined (Table 2). The structure model was refined with each of them using all the reflections collected. With the first four hypotheses (*A*, *B*, *C* and *D*), chromium was successively placed in one of the four possible sites. With the other hypotheses (*E*, *F* and *G*), Cr and Ti share the different proportions of all these four sites. Different parameters are taken into consideration in order to isolate the best hypothesis: wR_2, R_1, *S* (goodness-of-fit) and U_{eq} (isotropic displacements) of Li and Ti/Cr within the four sites in which they could be located.

It appears that two hypotheses, *E* and *F*, are significantly better than the others. However, owing to the closeness of the results (wR_2 = 0.0579 for *E* and 0.0655 for *F*) the choice still remains ambiguous.

A new reflection file containing only sensitive reflections was then prepared, in order to improve the contrast between the different Ti/Cr site-occupation models. The sensible reflection file is based on two extreme occupation hypotheses. According to the first one, chromium statistically occupies the fourfold sites (hypothesis *E*), while the second postulates that half of the eightfold sites are occupied by Cr (hypothesis *D*). F_c structure factors of all reflections were compared for the two models of cationic distribution. Then, only the most sensitive reflections for which

$$\frac{\Delta F_c^2}{\langle F_c^2 \rangle} \geq 0.1$$

were selected for the refinement.

The seven hypotheses were recalculated using 421 'sensitive' reflections within the whole measured *hkl* area (Table 1) and one of the solutions emerged as the best (Table 2). The *E* hypothesis seemed to be the most probable. As a result of this analysis, it

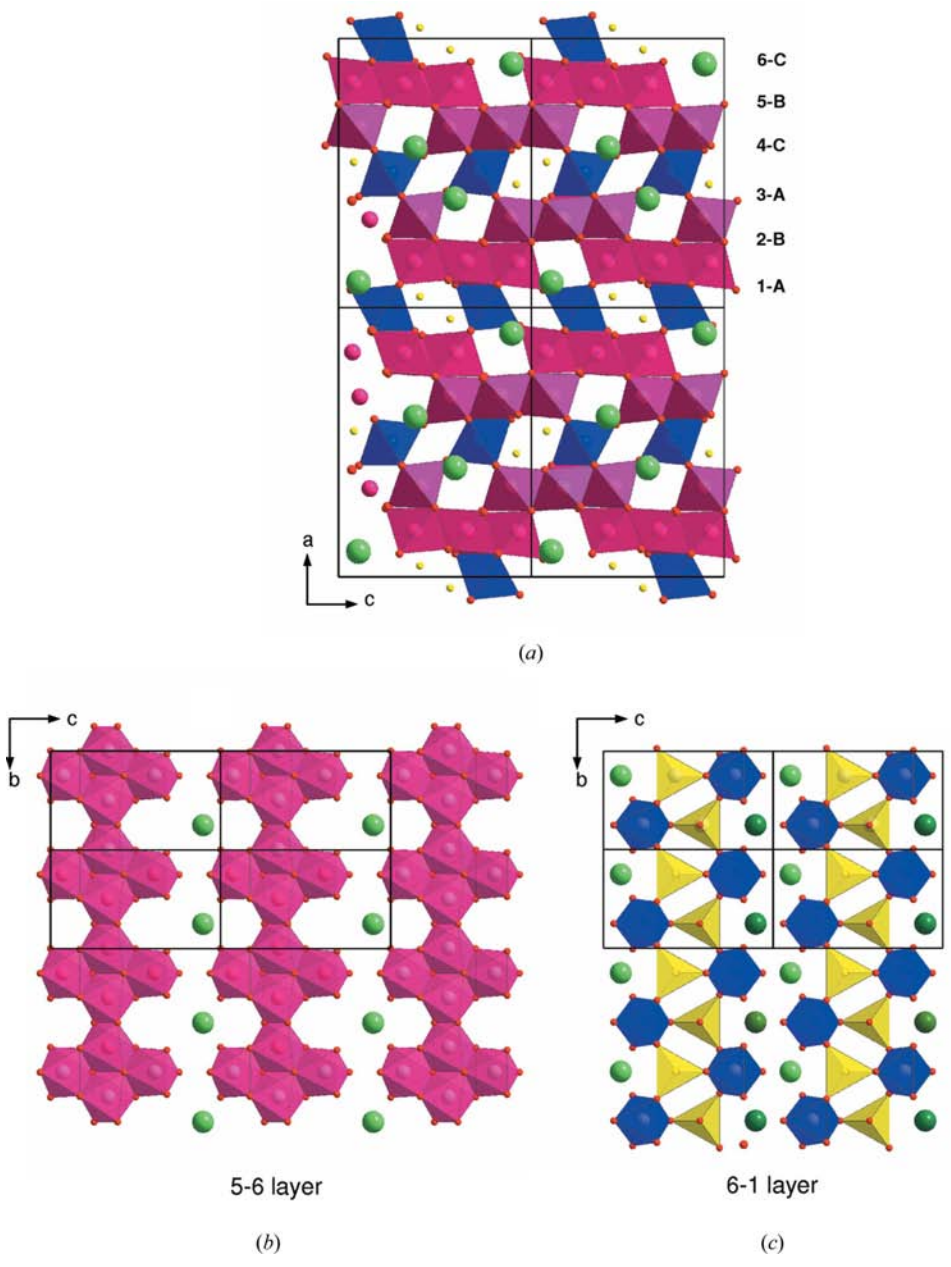

Figure 4
$SrLiCrTi_4O_{11}$ structure description with (M^*O_6) octahedra (red and blue), (LiO_4) tetrahedra (yellow) and Sr ions (green): (*a*) different sheet sequence along the *a* axis; (*b*) 5–6 (*B*–*C*) layer; (*c*) 6–1 (*C*–*A*) layer.

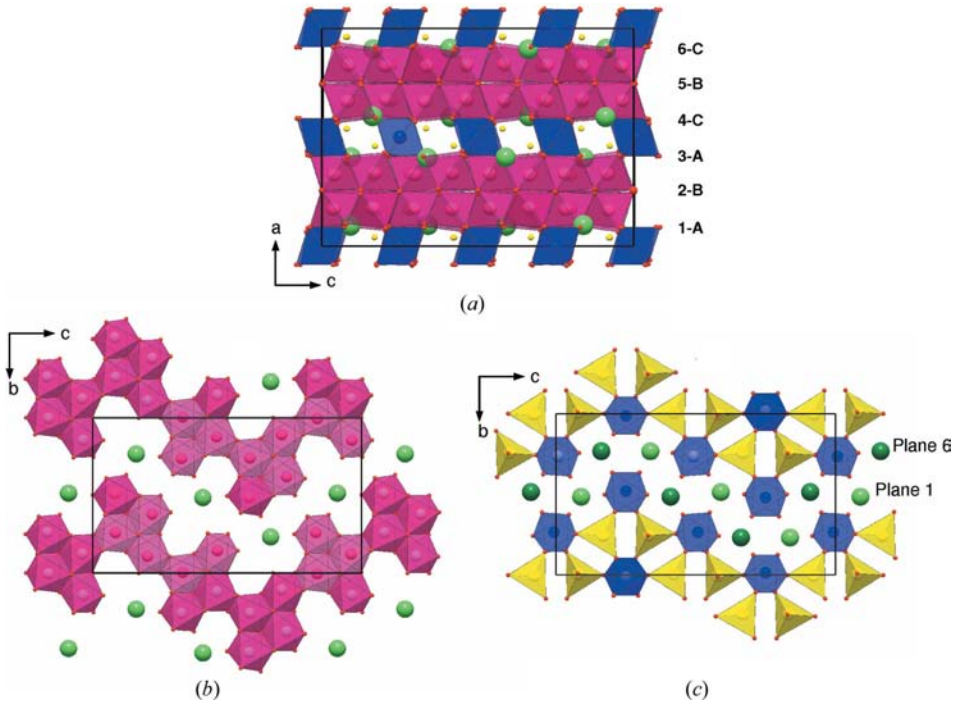

Figure 5
$SrLiFeTi_4O_{11}$ structure description with (Ti^*O_6) octahedra (red and blue), LiO_4 tetrahedra (yellow) and Sr ions (green): (*a*) different sheet sequence along the *a* axis; (*b*) 5–6 (*B*–*C*) layer; (*c*) 6–1 (*C*–*A*) layer.

can be concluded that Cr and Ti atoms statistically occupy each of the three fourfold sites (1/3Cr, 2/3Ti). The eightfold site is occupied by Ti atoms only. The refined atomic positions within this last model are summarized in Table 3.

3.2. Results with *Cr-prep*2

3.2.1. Neutron diffraction of powder *Cr-prep*2. As was shown in the previous paragraph, the structure refinement of $SrLiCrTi_4O_{11}$ using X-ray diffraction data was difficult, especially as far as the positions of the Cr and Ti atoms were concerned. Unlike X-rays, the neutron scattering lengths of titanium (−3.4 fm) and chromium (3.52 fm) are quite different (Bacon, 1975). A preliminary neutron powder-diffraction pattern simulation showed significant intensity variations of some peaks, especially at low angles, with respect to the different cationic distribution hypotheses (Fig. 1). Neutron powder-diffraction experiments were performed on the polycrystalline sample *Cr-prep*2 especially synthesized for this purpose.

Fig. 2 shows the final result of the Rietveld-type analysis of the neutron powder pattern. The presence of a small amount of $SrTiO_3$ in the sample was taken into account in the refinement process. The profile shape of the pattern was refined using a Thompson–Cox–Hastings pseudo-Voigt function (Finger *et al.*, 1994) and half-width parameters characterizing the instrumental resolution of the 3T2 diffractometer. The seven hypotheses for the Cr/Ti occupation of the four octahedral sites in $SrLiCrTi_4O_{11}$ were examined and the results of the refinements are summarized in Table 4. The two best refinements, *D* and *G*, converge with very similar agreement factors. Both hypotheses presuppose that Cr atoms mostly occupy the 8(*d*) site. However, the delocalization of a small fraction of the Cr over the 4(*c*) sites (hypothesis *G*) proved to be very beneficial, especially for the isotropic displacement factors B_{iso}, whose values became reasonably positive. The agreement factors were also slightly better.

The neutron powder diffraction result contradicts the conclusions drawn from the single-crystal X-ray diffraction of *Cr-prep*1.

3.2.2. Single-crystal X-ray diffraction of *Cr-prep*2. Optical examination of the *Cr-prep*2 powder sample showed the presence of single crystals with small dimensions which, however, were appropriate for X-ray diffraction. Thus, one of these crystals was selected and a complete structural determination was carried out under similar conditions to *Cr-prep*1 (Table 1). The seven possible Cr/Ti distributions over the four cationic sites were examined again. The results of the refinements using either the 'all reflections' file or a '*selected* reflections' file are almost identical. They reject the structural models *A*, *B*, *C* and *E*, *i.e.* all hypotheses which imply that Ti atoms only occupy the 8(*d*) site (Table 4). Furthermore, X-ray diffraction does not in fact allow any conclusions to be drawn concerning the exact Cr distribution (models *D*, *F* and *G*). Nevertheless, these results are quite consistent with the neutron diffraction performed with the same powder sample and confirm a different Cr/Ti site occupation in comparison with the *Cr-prep*1 sample.

3.3. Conclusion and structure description of $SrLiCrTi_4O_{11}$

As was shown above, *Cr-prep*1 and *Cr-prep*2 present two different Cr/Ti distributions. However, all the other structural parameters are almost identical (cell parameters, space groups and atomic coordinates). This discrepancy could be assigned to the thermal history of the samples. The *Cr-prep*1 crystals are grown in a flux with decreasing temperature in the range 1253–1173 K, whereas *Cr-prep*2 is obtained by a solid-state reaction at a higher temperature. Hence, depending on the conditions for the synthesis of $SrLiCrTi_4O_{11}$, the Cr- and Ti-atom distributions over the different crystallographic sites could differ. The structural model proposed in Table 3 is related to *Cr-prep*1 and hypothesis *E*.

The structure can be described by a close-packed arrangement of Sr and O atoms. The unit cell contains six 'compact

Table 5
Selected distances (in Å) for $SrLiCrTi_4O_{11}$ from *Cr-prep*1, refinement hypothesis *E*.

Sr—O		Li—O	
Sr—O8^{i}	2.646 (1)	Li—O1	1.920 (6)
Sr—O8^{ii}	2.646 (1)	Li—O4^{iii}	1.984 (7)
Sr—O6^{iv}	2.709 (1)	Li—O8^{ii}	2.011 (4)
Sr—O6^{v}	2.709 (1)	Li—O8^{i}	2.011 (4)
Sr—O3	2.741 (2)		
Sr—O5^{iii}	2.754 (2)		
Sr—O5^{ii}	2.933 (1)		
Sr—O5^{vi}	2.933 (1)		
Sr—O7^{iii}	2.943 (2)		
Sr—O7^{vii}	2.943 (2)		
Sr—O7^{ii}	3.105 (2)		
Sr—O7^{i}	3.105 (2)		
Ti*—O			
*M*1*—O5^{viii}	1.906 (2)	*M*3*—O5	1.893 (2)
*M*1*—O8^{viii}	1.95 (2)	*M*3*—O6^{ii}	1.948 (2)
*M*1*—O8^{ix}	1.950 (2)	*M*3*—O6^{i}	1.948 (2)
*M*1*—O7^{x}	1.969 (2)	*M*3*—O3	2.006 (2)
*M*1*—O7^{xi}	1.969 (2)	*M*3*—O7	2.042 (2)
*M*1*—O1	2.028 (2)	*M*3*—O7^{xii}	2.042 (2)
*M*2*—O8^{xii}	1.871 (2)	*M*4*—O2	1.933 (2)
*M*2*—O8	1.871 (1)	*M*4*—O1	1.939 (2)
*M*2*—O2	1.878 (2)	*M*4*—O3^{xi}	1.945 (2)
*M*2*—O4^{xiii}	1.992 (2)	*M*4*—O4^{xi}	1.963 (2)
*M*2*—O6^{xii}	2.159 (2)	*M*4*—O6^{ii}	1.979 (2)
*M*2*—O6	2.159 (2)	*M*4*—O7^{xi}	2.026 (2)

Symmetry codes: (i) $-x+\frac{1}{2}, y+\frac{1}{2}, z-\frac{1}{2}$; (ii) $-x+\frac{1}{2}, -y, z-\frac{1}{2}$; (iii) $x-\frac{1}{2}, y, -z+\frac{1}{2}$; (iv) $x, -y+\frac{1}{2}, z-1$; (v) $x, y, z-1$; (vi) $-x+\frac{1}{2}, -y+1, z-\frac{1}{2}$; (vii) $x-\frac{1}{2}, -y+\frac{1}{2}, -z+\frac{1}{2}$; (viii) $x-\frac{1}{2}, y, -z+\frac{3}{2}$; (ix) $x-\frac{1}{2}, -y+\frac{1}{2}, -z+\frac{3}{2}$; (x) $-x+\frac{1}{2}, y+\frac{1}{2}, z+\frac{1}{2}$; (xi) $-x+\frac{1}{2}, -y, z+\frac{1}{2}$; (xii) $x, -y+\frac{1}{2}, z$; (xiii) $x, y, z+1$. *M**: Ti/Cr mixture.

planes' perpendicular to [100] in the layer sequence *ABACBC* [(chc)$_2$] (Fig. 3*a*). The two pairs of symmetry-equivalent layers *A* and *C* contain seven O atoms per Sr atom (Fig. 3*b*), while the two equivalent *B* layers contain eight O atoms each.

This close-packed arrangement of 48 atoms in the unit cell leads to 48 octahedral sites, 20 of them involving one or two Sr atoms (16 with one Sr and four with two Sr). Only 20 of the 28 octahedral sites with six O atoms each are occupied by Ti/Cr (*M** later in the text). Moreover, Li atoms in the unit cell occupy four tetrahedral sites (with four O atoms) of the close packing.

This occupancy of octahedral and tetrahedral sites by *M** and Li atoms, respectively, leads to two types of polyhedral sheets, whose sequence along [100] can be seen in Fig. 4(*a*). The first *BC*-type sheet is presented in Fig. 4(*b*). It is constituted of chains along the *b* axis of edge-sharing *M**2, *M**3 and *M**4 octahedra (*M**2O$_6$ and *M**3O$_6$ border the *M**4O$_6$ rows). Two consecutive equivalent sheets along the *a* axis, translated by $(0, \frac{1}{2}, \frac{1}{2})$, form a double *CBC* (or *ABA*) sheet (Fig. 4*a*) with Sr atoms inserted into cavities of the upper and lower planes, respectively. In these 'double sheets' all *M**O$_6$ octahedra are linked by common edges.

The second sheet of the *CA* type is shown in Fig. 4(*c*). It contains chains of isolated *M**O$_6$ octahedra and isolated LiO_4 tetrahedra linked by corners. These chains as well as rows of Sr atoms run along the *b* axis.

Selected interatomic distances in $SrLiCrTi_4O_{11}$ are presented in Table 5.

The *M**O$_6$ octahedra are slightly distorted. However, the mean value of the *M**—O distance (⟨*M**—O⟩ 1.973 Å) is in rather good agreement with related distances in other titanates built of TiO_6 octahedra.

Li atoms are surrounded by four O atoms forming a tetrahedron which shares common corners with six *M**O$_6$ octahedra (⟨Li—O⟩ 1.982 Å).

Sr atoms are coordinated to 12 O atoms, six in their own compact plane, three in the upper compact plane and three in the lower compact plane. Sr—O distances range between 2.646 and 3.105 Å with a ⟨Sr—O⟩ mean value of 2.847 Å, in agreement with other compounds having a similar strontium coordination.

3.4. Comparison between $SrLiCrTi_4O_{11}$ and $Ba_2Li_3Ti_{9.25}O_{22}$ structures

Taking into account the axis permutation between *Pnma* and *Pmcn* space groups and the origin translation $(0, \frac{1}{2}, \frac{1}{2})$, as indicated above in §2.2, a close similarity in atomic arrangement was observed between the chromium-containing titanate under consideration and the Tillmanns' compound, $Ba_2Li_3Ti_{9.25}O_{22}$ (*T* compound in the following; Tillmanns & Wendt, 1976).

The same packing sequences of compact planes containing O and Ba atoms (*ABACBC* [(chc)$_2$]) exist. The principal difference appears with the supplementary Li atoms in $Ba_2Li_3Ti_{9.25}O_{22}$, which induce some titanium vacancies. Three half-occupied fourfold sites have been found for lithium in the *T* compound, two octahedral and one tetrahedral. In $SrLiCrTi_4O_{11}$, only Li2 isolated tetrahedra are observed and the site is fully occupied.

In fact, the *T* compound appears to be a variation of the more simple structural model of $SrLiCrTi_4O_{11}$. In this compound compensation for the absence of M^{III} ions in Ti sites is achieved by titanium vacancies and the insertion of supplementary Li ions in the close-packing arrangement.

4. Crystal structure of $SrLiFeTi_4O_{11}$

4.1. Solution with single-crystal X-ray diffraction

The presence of iron instead of chromium in the $SrLiMTi_4O_{11}$ compound was found to lead to an important structure evolution. Thus, the $SrLiFeTi_4O_{11}$ unit cell proved to be four times larger than that of $SrLiCrTi_4O_{11}$ ($a_{Fe} = a_{Cr}$, $b_{Fe} = 2b_{Cr}$, $c_{Fe} = 2c_{Cr}$). Structure determination was carried out by Patterson function deconvolution in the *Pbcn* space group (see Table 1). In the $SrLiFeTi_4O_{11}$ structure, Fe and Ti atoms occupy 11 crystallographic sites: nine eightfold and two fourfold. Different site-occupation hypotheses have been tried for structure solution and refinement. The best results are obtained with the hypothesis assuming a statistical distribution of Fe and Ti atoms in the 11 sites (80% Ti and 20% Fe). In the periodic table of elements iron is further from titanium than chromium is, so the difference between the X-ray scattering

Table 6
Atomic positions and U_{eq} for $SrLiFeTi_4O_{11}$, refinement hypothesis *F*.

Atoms	Site	Site symmetry	*x*	*y*	*z*	U_{eq} (Å^2)
0.8Ti1/0.2Fe1	4(*c*)	.2.	0	0.01487 (10)	1/4	0.0101 (2)
0.8Ti2/0.2Fe2	4(*c*)	.2.	0	0.48027 (10)	1/4	0.0089 (2)
0.8Ti3/0.2Fe3	8(*d*)	1	0.00100 (5)	0.26536 (7)	0.49253 (4)	0.0091 (2)
0.8Ti4/0.2Fe4	8(*d*)	1	0.16459 (6)	0.26122 (7)	0.17009 (4)	0.0072 (1)
0.8Ti5/0.2Fe5	8(*d*)	1	0.16516 (5)	0.48780 (6)	0.41829 (3)	0.0055 (1)
0.8Ti6/0.2Fe6	8(*d*)	1	0.17395 (6)	0.12221 (6)	0.03889 (4)	0.0081 (1)
0.8Ti7/0.2Fe7	8(*d*)	1	0.32537 (6)	0.49505 (6)	0.16476 (4)	0.0112 (2)
0.8Ti8/0.2Fe8	8(*d*)	1	0.32727 (6)	0.39129 (6)	0.29695 (4)	0.0088 (1)
0.8Ti9/0.2Fe9	8(*d*)	1	0.33029 (6)	0.24050 (6)	0.41530 (3)	0.0084 (1)
0.8Ti10/0.2Fe10	8(*d*)	1	0.33155 (6)	0.35537 (6)	0.03622 (4)	0.0099 (1)
0.8Ti11/0.2Fe11	8(*d*)	1	0.33166 (5)	0.12154 (6)	0.27915 (3)	0.0080 (1)
O1	8(*d*)	1	0.0641 (2)	0.3885 (3)	0.4494 (2)	0.0096 (6)
O2	8(*d*)	1	0.0703 (2)	0.3643 (3)	0.2011 (2)	0.0102 (9)
O3	8(*d*)	1	0.0810 (3)	0.1268 (3)	0.2062 (2)	0.0110 (6)
O4	8(*d*)	1	0.0840 (2)	0.0006 (2)	0.3286 (1)	0.0077 (5)
O5	8(*d*)	1	0.0851 (2)	0.1445 (3)	0.4607 (1)	0.0074 (6)
O6	8(*d*)	1	0.0861 (3)	0.2434 (3)	0.0825 (1)	0.0082 (5)
O7	8(*d*)	1	0.2386 (2)	0.1292 (3)	0.1251 (1)	0.0056 (6)
O8	8(*d*)	1	0.2444 (2)	0.3759 (3)	0.1230 (1)	0.0073 (6)
O9	8(*d*)	1	0.2448 (2)	0.3672 (3)	0.3750 (1)	0.0081 (6)
O10	8(*d*)	1	0.2452 (2)	0.2503 (2)	0.2501 (2)	0.0061 (7)
O11	8(*d*)	1	0.2480 (2)	0.0011 (2)	0.2478 (2)	0.0064 (8)
O12	8(*d*)	1	0.2550 (2)	0.2515 (2)	0.4970 (2)	0.0072 (8)
O13	8(*d*)	1	0.2565 (2)	0.0030 (2)	0.00005 (17)	0.0082 (8)
O14	8(*d*)	1	0.2630 (2)	0.1164 (3)	0.3733 (1)	0.0064 (6)
O15	8(*d*)	1	0.3976 (2)	0.4902 (3)	0.0782 (1)	0.0062 (6)
O16	8(*d*)	1	0.3976 (2)	0.2543 (2)	0.3288 (1)	0.0052 (6)
O17	8(*d*)	1	0.4103 (2)	0.3934 (3)	0.2144 (1)	0.0063 (5)
O18	8(*d*)	1	0.4109 (2)	0.0012 (2)	0.3258 (2)	0.0080 (6)
O19	8(*d*)	1	0.4129 (2)	0.3543 (3)	0.4635 (1)	0.0060 (5)
O20	8(*d*)	1	0.4135 (2)	0.2439 (2)	0.0717 (2)	0.0067 (6)
O21	8(*d*)	1	0.4173 (2)	0.1083 (3)	0.2105 (1)	0.0065 (5)
O22	8(*d*)	1	0.4173 (2)	0.1245 (3)	0.4540 (1)	0.0086 (8)
Sr1	8(*d*)	1	0.09606 (3)	0.23258 (4)	0.33789 (2)	0.0125 (1)
Sr2	8(*d*)	1	0.40740 (3)	0.01442 (4)	0.08996 (2)	0.0114 (1)
Li1	8(*d*)	1	0.4593 (6)	0.2561 (6)	0.1682 (4)	0.012 (2)
Li2	8(*d*)	1	0.4606 (5)	0.4951 (5)	0.4221 (3)	0.002 (1)

factors leads to a more unambiguous conclusion in the case of an iron-containing titanate.

Atomic coordinates, isotropic equivalent displacement parameters and selected interatomic distances are presented in Tables 6 and 7.

4.2. Description of the $SrLiFeTi_4O_{11}$ structure and filiation with the structure of the chromium-containing compound

As in the case of chromium-containing titanate, the structure of $SrLiFeTi_4O_{11}$ can be described by a close-packing arrangement of Sr and O atoms, with the same *ABACBC* [$(chc)_2$] sequence perpendicular to [100] (Fig. 3*c*). Here the four symmetry-equivalent layers *A* and *C* contain 28 O atoms and four Sr atoms (Fig. 3*d*), while the two equivalent *B* layers possess 32 O atoms each. It is worth comparing the atomic distribution in the Sr/O close-packing sheets in $SrLiCrTi_4O_{11}$ (Fig. 3*b*) and $SrLiFeTi_4O_{11}$ (Fig. 3*d*). One can clearly see why the iron-containing compound adopts a four times larger unit cell and still keeps the same 1/7 atomic ratio.

In $SrLiFeTi_4O_{11}$ two types of sheets perpendicular to [100] are also observed (Fig. 5*a*). The *BC* sheet presented in Fig. 5(*b*) contains 32 octahedral sites (20 O_6 and 12 O_5Sr) and 64 tetrahedral sites; 16 octahedral O_6 sites are occupied by Ti/Fe atoms.

Two consecutive sheets along the *a* axis, translated by $(0, \frac{1}{2}, 0)$, constitute a doubled *CBC* (or *ABA*) sheet (Fig. 5*a*) with Sr atoms inserted in cavities of upper and lower planes and doing similar 'zigzag lines' along the *c* axis (Figs. 5*b* and *c*).

In the *CA* sheet (Fig. 5*c*), isolated TiO_6 octahedra are joined by corners with isolated LiO_4 tetrahedra doing the same 'zigzag lines' along the *c* axis as in the case of Sr atoms.

Thus, comparison between $SrLiCrTi_4O_{11}$ and $SrLiFeTi_4O_{11}$ structures shows that:

(i) the same close-packing arrangement with Sr—O compact planes is present in both titanates;

(ii) replacement of the Cr^{3+} ion with $r_{Cr}^{3+} = 0.615$ Å (CN = 6) [which is close to $r_{Ti}^{4+} = 0.605$ Å (CN = 6)] by the larger high-spin Fe^{3+} ion with $r_{Fe}^{3+} = 0.645$ Å (CN = 6), induces a different distribution of Sr and Li atoms, and a lowering of the symmetry (double values for cell parameters *b* and *c*).

5. Conclusion

Two new complex titanates, $SrLiCrTi_4O_{11}$ and $SrLiFeTi_4O_{11}$, were synthesized and their crystal structures were determined by single-crystal X-ray diffraction. A detailed crystallographic study of two different chemical preparations of the first compound, performed with a sensible reflection file and refinement of a neutron powder diffraction pattern, allowed the distinction between two different Cr- and Ti-atom distributions in the crystallographic sites of the samples having the same composition, but different chemical histories.

The structure established for $SrLiCrTi_4O_{11}$ was compared with the similar $Ba_2Li_3Ti_{9.25}O_{22}$ structure, reported previously by Tillmanns & Wendt (1976), as well as with the structure of the newly prepared $SrLiFeTi_4O_{11}$ titanate in which quite different compact (Sr—O) planes were found. The structures exhibited close-packed oxygen lattices with Sr atoms replacing O atoms and titanium, chromium or iron, and lithium occupying the interstitials.

It has been established that the close-packed lattices are based on a hexagonal unit cell, with layers having a thickness of 2.30 Å (the *a* parameter divided by the number of layers) and a hexagonal-plane base parameter of the order of 5.75 Å. Strontium sites plus the ordering of cations (Ti, Cr or Fe and Li) in interstitials reduce the symmetry from hexagonal to orthorhombic with changes in the in-plane lattice parameters

Table 7
Selected bond distances (Å) for $SrLiFeTi_4O_{11}$, refinement hypothesis *F*.

*M**: Ti/Fe mixture.

Ti*—O				Sr—O			
*M*1*—O3	1.917 (3)	*M*7*—O17	1.931 (4)	Sr1—O5	2.648 (3)	Sr2—O21	2.633 (3)
*M*1*—O3^{i}	1.917 (3)	*M*7*—O11^{ii}	1.940 (3)	Sr1—O4	2.678 (3)	Sr2—O20	2.663 (3)
*M*1*—O4	1.957 (3)	*M*7*—O7^{ii}	1.946 (3)	Sr1—O9	2.683 (3)	Sr2—O8^{iii}	2.721 (3)
*M*1*—O4^{i}	1.957 (3)	*M*7*—O8	1.956 (3)	Sr1—O10	2.715 (3)	Sr2—O1^{iv}	2.727 (3)
*M*1*—O17^{v}	2.000 (3)	*M*7*—O15	1.992 (3)	Sr1—O14	2.765 (3)	Sr2—O13	2.757 (3)
*M*1*—O17^{iii}	2.000 (3)	*M*7*—O3^{ii}	2.159 (4)	Sr1—O2^{i}	2.867 (4)	Sr2—O7	2.777 (3)
				Sr1—O3^{i}	2.878 (4)	Sr2—O2^{iii}	2.820 (3)
*M*2*—O2	1.917 (3)	*M*8*—O4^{ii}	1.868 (3)	Sr1—O1	2.886 (3)	Sr2—O22^{vi}	2.878 (4)
*M*2*—O2^{i}	1.917 (3)	*M*8*—O11^{ii}	1.908 (3)	Sr1—O3	2.894 (3)	Sr2—O18^{vi}	3.031 (4)
*M*2*—O18^{ii}	1.964 (3)	*M*8*—O9	1.948 (3)	Sr1—O6^{i}	2.984 (4)	Sr2—O1^{vii}	3.035 (3)
*M*2*—O18^{viii}	1.964 (3)	*M*8*—O16	1.957 (3)	Sr1—O18^{ii}	3.098 (3)	Sr2—O6^{iii}	3.120 (3)
*M*2*—O21^{viii}	2.024 (3)	*M*8*—O17	2.006 (3)	Sr1—O2	3.135 (3)	Sr2—O22^{ix}	3.142 (3)
*M*2*—O21^{ii}	2.024 (3)	*M*8*—O10	2.189 (3)				
				Li—O			
*M*3*—O1	1.872 (3)	*M*9*—O14	1.899 (3)	Li1—O17	1.944 (9)	Li2—O19	1.932 (7)
*M*3*—O5	1.922 (3)	*M*9*—O12	1.935 (3)	Li1—O21	1.984 (8)	Li2—O4^{ii}	1.961 (7)
*M*3*—O6^{i}	1.937 (3)	*M*9*—O22	1.956 (3)	Li1—O16^{vi}	1.986 (9)	Li2—O15^{vi}	1.969 (8)
*M*3*—O20^{x}	1.974 (3)	*M*9*—O16	1.965 (3)	Li1—O20	2.026 (9)	Li2—O5^{ii}	1.985 (7)
*M*3*—O22^{xi}	2.020 (3)	*M*9*—O19	1.986 (3)				
*M*3*—O19^{xi}	2.037 (3)	*M*9*—O9	2.042 (3)				
*M*4*—O2	1.869 (3)	*M*10*—O20	1.853 (3)				
*M*4*—O10	1.949 (3)	*M*10*—O12^{vii}	1.887 (3)				
*M*4*—O8	1.960 (3)	*M*10*—O5^{vii}	1.896 (3)				
*M*4*—O7	2.039 (3)	*M*10*—O15	1.985 (3)				
*M*4*—O3	2.061 (3)	*M*10*—O8	2.120 (3)				
*M*4*—O6	2.064 (3)	*M*10*—O13^{ii}	2.211 (3)				
*M*5*—O1	1.911 (3)	*M*11*—O21	1.816 (3)				
*M*5*—O13^{x}	1.959 (3)	*M*11*—O11	1.912 (3)				
*M*5*—O9	1.971 (3)	*M*11*—O10	1.991 (3)				
*M*5*—O14^{ii}	1.995 (3)	*M*11*—O18	1.995 (3)				
*M*5*—O22^{ii}	2.069 (3)	*M*11*—O16	2.035 (3)				
*M*5*—O18^{ii}	2.127 (3)	*M*11*—O14	2.101 (3)				
*M*6*—O7	1.936 (3)						
*M*6*—O19^{vii}	1.943 (3)						
*M*6*—O12^{vii}	1.943 (3)						
*M*6*—O13	1.945 (3)						
*M*6*—O15^{iii}	1.975 (3)						
*M*6*—O6	2.044 (3)						

Symmetry codes: (i) $-x, y, -z+\frac{1}{2}$; (ii) $-x+\frac{1}{2}, y+\frac{1}{2}, z$; (iii) $-x+\frac{1}{2}, y-\frac{1}{2}, z$; (iv) $x+\frac{1}{2}, y-\frac{1}{2}, -z+\frac{1}{2}$; (v) $x-\frac{1}{2}, y-\frac{1}{2}, -z+\frac{1}{2}$; (vi) $-x+1, y, -z+\frac{1}{2}$; (vii) $-x+\frac{1}{2}, -y+\frac{1}{2}, z-\frac{1}{2}$; (viii) $x-\frac{1}{2}, y+\frac{1}{2}, -z+\frac{1}{2}$; (ix) $x, -y, z-\frac{1}{2}$; (x) $-x+\frac{1}{2}, -y+\frac{1}{2}, z+\frac{1}{2}$; (xi) $x-\frac{1}{2}, -y+\frac{1}{2}, -z+1$.

(*b* and *c* in the case under consideration). Here the role of Li atoms which occupy only tetrahedral sites is emphasized.

The two novel compounds which are the subject of the present work can be considered as new members of the alkaline earth polytitanate family described by Tillmanns *et al.* (1985). Similar close-packed lattices have been encountered in the $BaO–Fe_2O_3–TiO_2$ system with more complex layer stacking (Siegrist & Vanderah, 2003).

Detailed studies on the magnetic and electronic properties of the new compounds are now in progress and will be the subject of future communications.

References

Arillo, M. A., López, M. L., Fernández, M. T., Veiga, M. L. & Pico, C. (1996). *J. Solid State Chem.* **125**, 211–215.

Arillo, M. A., López, M. L., Perez-Cappe, E., Pico, C. & Veiga, M. L. (1998). *Solid State Ion.* **107**, 307–312.

Bacon, G. E. (1975). *Neutron Diffraction*, 3rd Ed. Oxford: Clarendon Press.

Belharouak, I. & Amine, K. (2003). *Electrochem. Commun.* **5**, 435–438.

Bhalla, A. S., Guo, R. & Roy, R. (2000). *Mater. Res. Innovat.* **4**, 3–26.

Chen, C., Spears, M., Wondre, F. & Ryan, J. (2003). *J. Cryst. Growth*, **250**, 139–145.

Dorrian, J. F. & Newnham, R. E. (1969). *Mater. Res. Bull.* **4**, 179–183.

Dussarat, C., Howie, R. A., Mather, G. C., Torres-Martinez, L. M. & West, A. R. (1997). *J. Mater. Chem.* **7**, 2103–2106.

Finger, L. W., Cox, D. E. & Jephcoat, A. P. (1994). *J. Appl. Cryst.* **27**, 892–900.

Garcia-Alvarado, F., Martin-Gil, M. & Kuhn, A. (2003). *Mater. Res. Soc. Symp. Proc.* **756**, 255–260.

Goldschmidt, V. M. (1927). *Geochemische Verteilungsgesetze der Elemente.* Oslo: Norske Videnskap.

Gunawardane, R. P., Fletcher, J. G., Dissanayake, M. A. K. L., Howie, R. A. & West, A. R. (1994). *J. Solid State Chem.* **112**, 70–72.

Izquierdo, G. & West, A. R. (1980). *Mater. Res. Bull.* **15**, 1655–1660.

Kajiyama, A., Takada, K., Arihara, K., Inada, T., Sasaki, H., Kondo, S. & Watanabe, M. (2003). *J. Electrochem. Soc.* **150**, A157–A160.

Koseva, I., Chaminade, J.-P., Gravereau, P., Pechev, S., Peshev, P. & Etourneau, J. (2005). *J. Alloys Compd*, **389**, 47–54.

Koseva, I., Peshev, P., Pechev, S., Gravereau, P. & Chaminade, J.-P. (2002). *Z. Naturforsch. Teil B*, **57**, 512–518.

Martin, P., López, M. L., Veiga, M. L. & Pico, C. (2004). *Solid State Sci.* **6**, 325–331.

Mikkelsen Jr, J. C. (1980). *J. Am. Ceram. Soc.* **63**, 331–335.

Morosin, B. & Mikkelsen, J. C. (1979). *Acta Cryst.* B**35**, 798–800.

Nonius BV (1999). *COLLECT*. Nonius BV, Delft, The Netherlands.

Nonobe, E., Yamazaki, Y., Shimura, T., Kanno, R. & Iwahara, H. (2003). *Solid State Ion.* **156**, 35–43.

Otwinowski, Z. & Minor W. (1997). *Methods in Enzymology*, Vol. 276, *Macromolecular Crystallography*, Part A, edited by C. W. Carter & R. M. Sweet. London: Academic Press.

Robertson, A. D., Trevino, L., Tukamoto, H. & Irvine, J. T. S. (1999). *J. Power Sources*, **81–82**, 352–357.

Robertson, A. D., Tukamoto, H. & Irvine, J. T. S. (1999). *J. Electrochem. Soc.* **146**, 3958–3962.

Rodriguez-Carvajal, J. (1990). *Powder Diffraction.* Proc. of the Satellite Meeting of the 15th Congress of IUCr, p. 127. Toulouse, France.

Roisnel, T. & Rodriguez-Carvajal, J. (2001). *Mater. Sci. Forum*, **378–381**, 118–123.

Roy, R. (1954). *J. Am. Ceram. Soc.* **37**, 581–588.

Sebastian, L. & Gopalakrishnan (2003). *J. Solid State Chem.* **172**, 171–177.

Sheldrick, G. M. (1997*a*). *SHELXS*97. University of Göttingen, Germany.

Sheldrick, G. M. (1997*b*). *SHELXL*97. University of Göttingen, Germany.
Siegrist, T. & Vanderah, T. A. (2003). *Eur. J. Inorg Chem.* **2003**, 1483–1501.
Sun, Y.-K., Jung, D.-J., Lee, Y. S. & Nahm, K. S. (2004). *J. Power Sources*, **125**, 242–245.
Tabuchi, M., Nakashima, A., Shigemura, H., Ado, K., Kobayashi, H., Sakaebe, H., Tatsumi, K., Kageyama, H., Nakamura, T. & Kanno, R. (2003). *J. Mater. Chem.* **13**, 1747–1757.
Tillmanns, E., Hofmeister, W. & Baur, W. H. (1985). *J. Solid State Chem.* **58**, 14–28.
Tillmanns, E. & Wendt, I. (1976). *Z. Kristallogr.* **144**, 16–31.
Torres-Martinez, L. M., Suckut, C., Jimenez, R. & West, A. R. (1994). *J. Mater. Chem.* **4**, 5–8.
Wersing, W. (1996). *Curr. Opin. Solid State Mater. Sci.* **1**, 715–731.
West, A. R. (1994). Editor. *Solid State Chemistry and its Application.* New York: John Wiley and Sons, Ltd.
Zheng, W. J., Okuyama, R., Esaka, T. & Iwahara, H. (1989). *Solid State Ion.* **35**, 235–239.